II. RADIO ASTRONOMY*

Prof. A. H. Barrett	J. I. Glaser	A. E. E. Rogers
Prof. J. W. Graham	J. W. Kuiper	J. H. Spoor
Prof. R. P. Rafuse	W. B. Lenoir	D. H. Staelin
R. J. Allen	J. M. Moran, Jr.	D. H. Steinbrecher
R. K. Breon	M. A. Palfy	W. J. Wilson

A. OBSERVATIONS OF MICROWAVE EMISSION FROM ATMOSPHERIC OXYGEN

1. Introduction

The theoretical development of microwave emission from molecular oxygen in the atmosphere indicates that studies of its resonance lines afford a new and competitive means of probing the physical structure of the atmosphere. This report covers the second year of a program with the following objectives:

1. To experimentally verify the theoretical predictions through observations from a balloon.

2. To design and perfect spectral-line radiometers for spacecraft operation at approximately 5-mm wavelength.

A program to measure thermal emission from the molecular oxygen line and to determine its linewidth, intensity, and dependence on antenna zenith angle was undertaken. The system built for this purpose is a Dicke superheterodyne radiometer operating at 61.1506 Gc. Three IF amplifiers, having center frequencies 20, 60, and 200 Mc, with bandwidths 10, 10, and 15 Mc, respectively, are time-shared with the low-frequency amplifiers, synchronous detector, and recorder. As the system takes advantage of the symmetry of the resonance line, no image rejection is employed. This system has previously been described in detail.[1]

2. Balloon Flights

In the second year of this program four balloon flight experiments have been performed.

Figure II-1 shows the flight profile for all four flights. There were 2 hours of ascent to 30 km, 3 hours of float, 1 3/4 hours of valved descent to 5 km, and 1/4 hour of parachute to ground.

Flight 32P (Balloon Base nomenclature) on 6 February 1964, yielded no data because of tape recorder malfunctions.

Flight 33P (9 February 1964) yielded 2 1/2 hours of data. After 2 1/2 hours, the

*This work was supported in part by the National Aeronautics and Space Administration (Grants NsG-240-62 and NsG-419); and in part by Purchase Order DDL BB-107 with Lincoln Laboratory, a center for research operated by Massachusetts Institute of Technology, with the support of the U.S. Air Force under Contract AF 19(628)-500; and in part by the Office of Naval Research (Contract Nonr 3963(02).

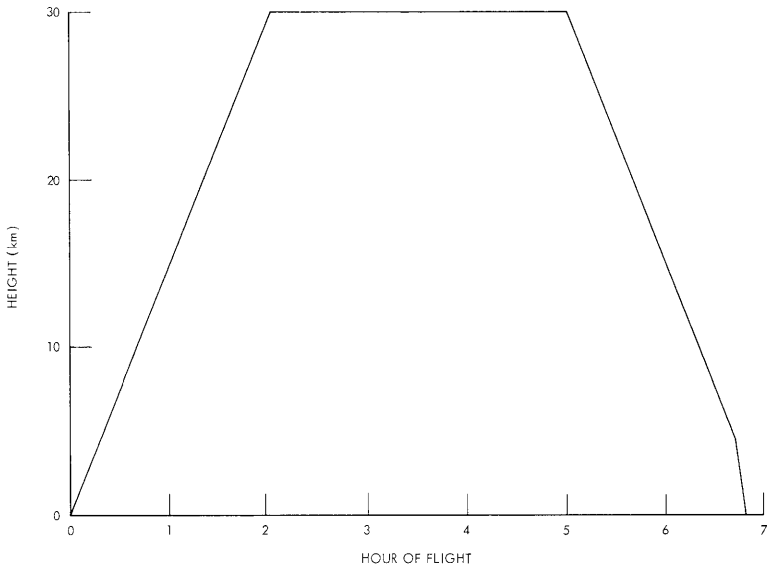

Fig. II-1. Flight profile.

oil used to cool the klystron began to leak into the waveguide and attenuated the local-oscillator signal into the mixer to the extent that no signal output was detectable.

Flight 55P (23 July 1964) yielded data from two of the three channels for 3 hours and from the other channel for 1 hour. Temperature changes caused the gain of the 60-Mc IF amplifier to increase until after 1 hour the signals from that channel saturated the tape recorder. Insufficient charge in the tape-recorder batteries caused their voltage to drop below the operating level of the recorder after 3 hours of flight.

Flight 57P (28 July 1964) yielded no data after launch because of an open circuit in a tape-recorder connection.

3. Flight Radiometer

The multichannel radiometer[1] has undergone progressive refinement as data from the flights suggested useful modification. Figure II-2 shows the block diagram of the most recent system.

Before Flight 32P an isolator was added ahead of the balanced mixer to reduce the effects of the changing VSWR. A second slightly cooler reference load was included for additional calibration of the radiometer in flight.

The programming was then changed to a twelve-position program with a minute on each of four inputs: 60° zenith angle, low-temperature calibration load, high-temperature calibration load, and 75° zenith angle. This sequence was measured while connected to each of three IF channels.

The data from Flight 33P indicated that cooling oil was forcing itself past the O-ring

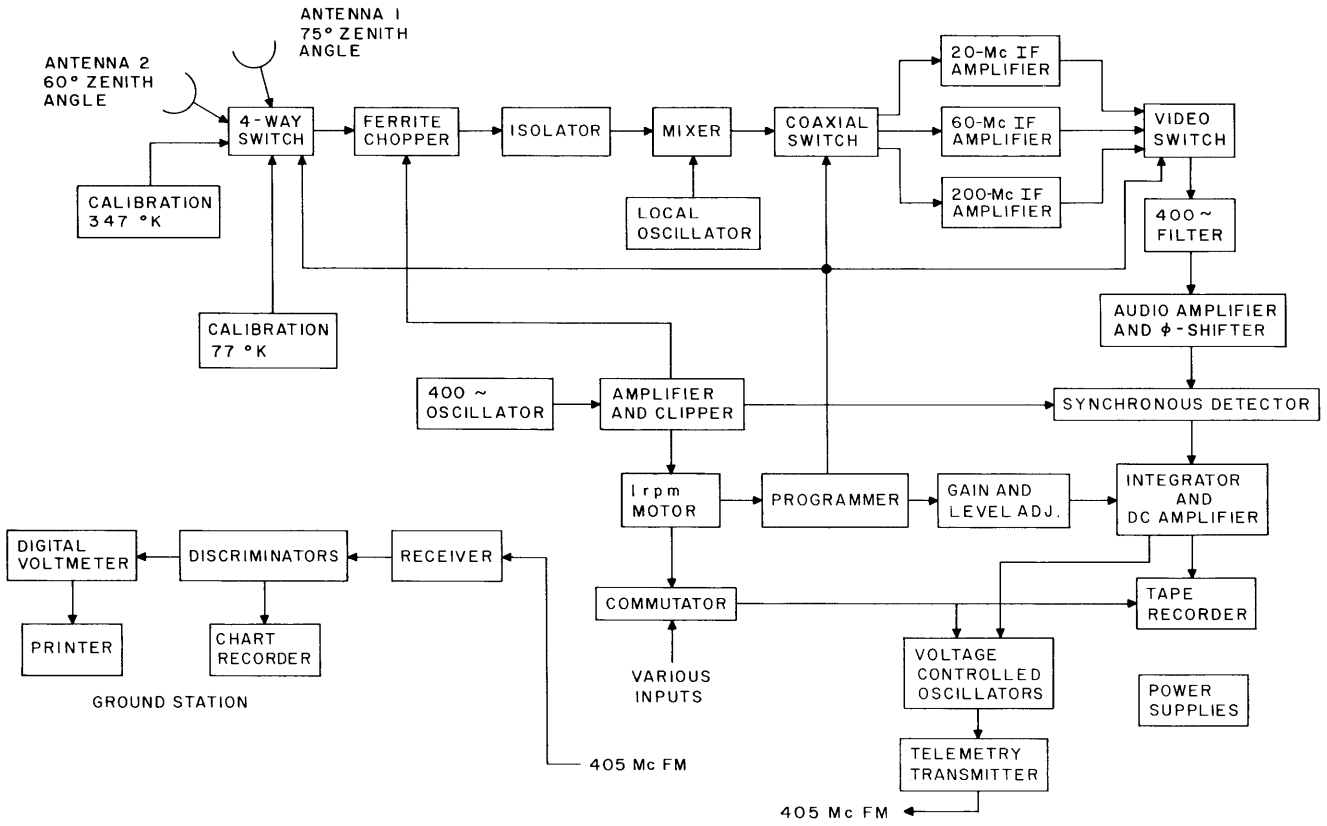

Fig. II-2. Flight radiometer.

seals into the local-oscillator waveguide. After this flight, the klystron power supply was completely rebuilt, incorporating changes such as a current-regulated filament supply, a filament overvoltage protection, a self-contained mode sweeping for tune-up, elimination of the batteries in the stabilizer circuit, and a better sealing of the waveguide joints from oil penetration.

To increase the accuracy of calibration, the cooler calibration load was replaced by a load cooled by liquid nitrogen.

As one of the major difficulties has been the recovery of data, the system is being modified to accept telemetry. The data rate of our experiment is sufficiently low (a reading every two seconds is adequate) that a digital voltmeter and printer can be used to record the telemetered data and at the same time increase the reading accuracy.

Using a 400-cycle tuning fork, we have developed a time-stable signal to drive a 1-rpm synchronous motor. This motor turns the 30-segment commutator and also actuates the programmer, producing a synchronized data channel which can handle all data on one voltage-controlled oscillator (VCO) channel. Because the tuning fork is stable to 1 part in 10^4, it is possible to derive the synchronizing pulses at the ground station from the line frequency.

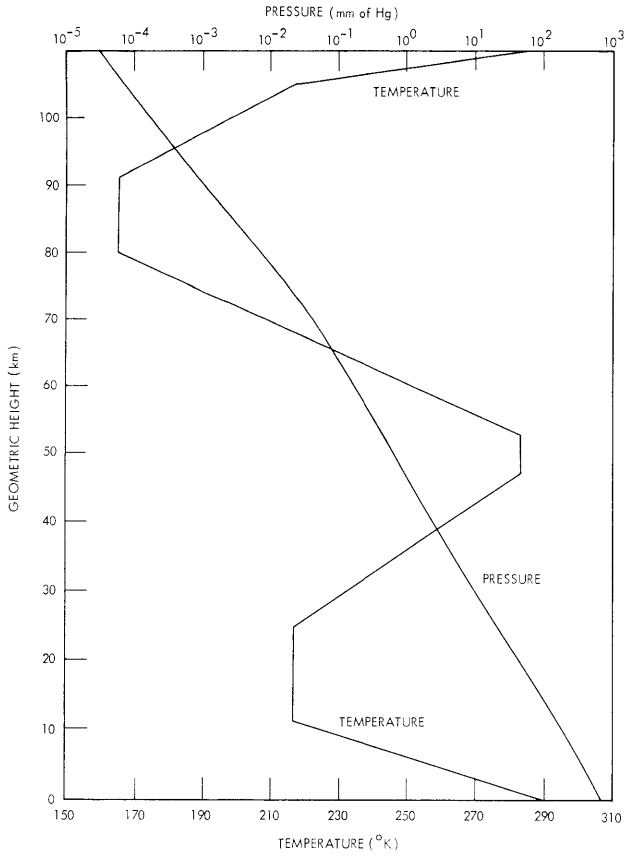

Fig. II-3. ARDC model atmosphere.

On future flights an additional VCO channel will also be used to record the analog or integrated radiometer output on a strip chart recorder.

On the most recent flights (55P and 57P) the only item not completed in time was the telemetry transmitter.

4. Data Analysis and Results

a. Theoretical Calculations

All theoretical calculations are made under the assumption that the physical structure of the atmosphere is adequately modeled by the ARDC standard atmosphere. The temperature and pressure profiles of this model are shown in Fig. II-3.

The equation of radiative transfer is integrated (IBM 7094 Computer) by using the above-mentioned temperatures and pressures to give the brightness

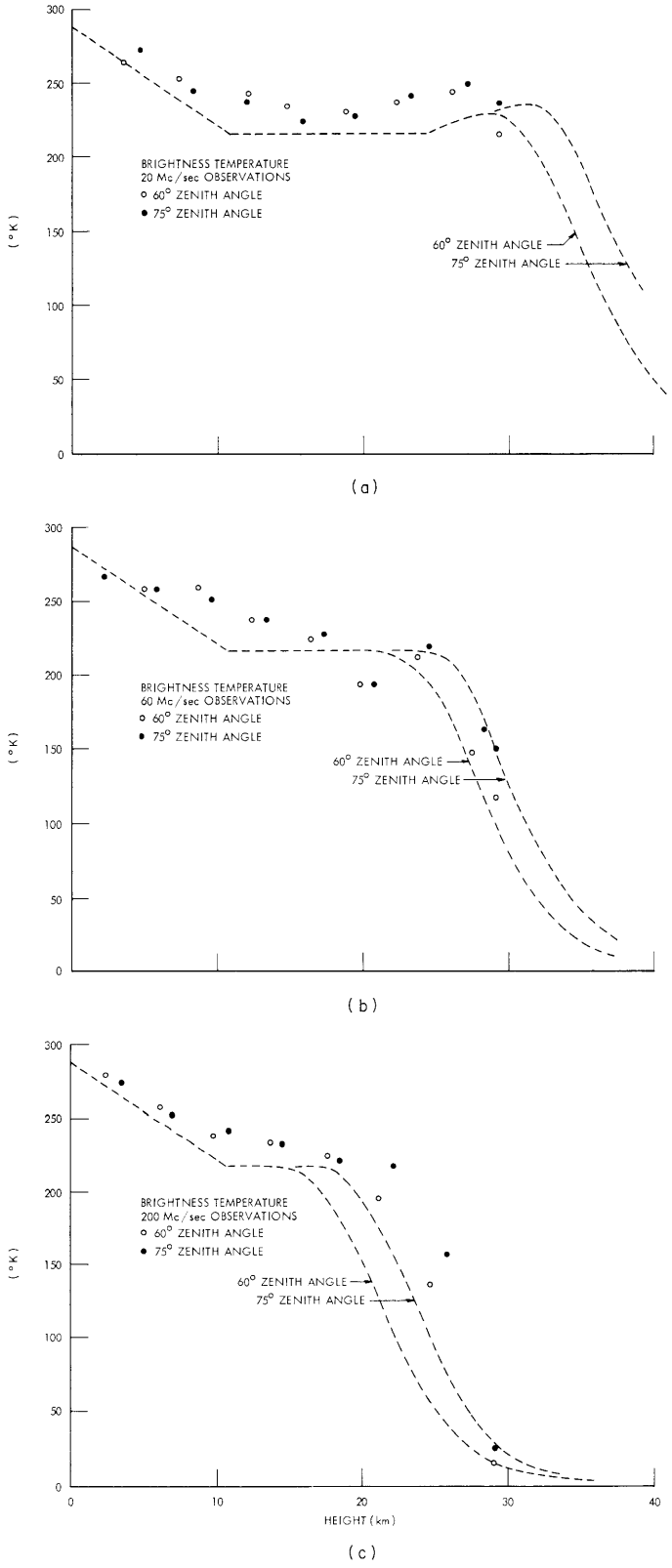

Fig. II-4. Brightness temperature.

temperature for a given frequency, zenith angle, and height of observation.

b. Results of Flight 33P

Useful data were obtained for the first 2 1/2 hours of the flight. The complete ascent and 40 minutes of the float are covered by these data.

Figure II-4 shows the measured brightness temperatures plotted against height. The theoretical calculations are shown as dotted lines. The last plotted points at float height (31.2 km) represent the average of the six measurements taken at float. Figure II-5 shows

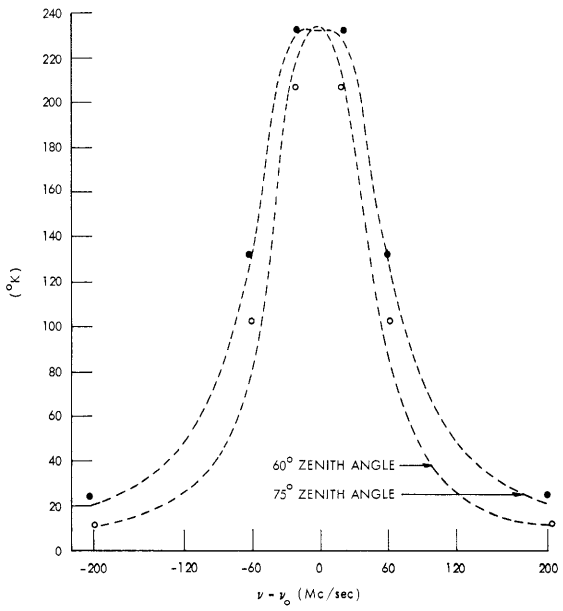

Fig. II-5. Brightness temperature measured at 30 km.

these points plotted against frequency on the theoretical line shape.

As indicated earlier, the method of obtaining the calibration temperatures on this flight causes the rms error of one measurement to depend heavily on the brightness temperature measured. The rms error is ~5°K at 300°K brightness temperature and 50°K at 0°K brightness temperature, with a linear relation between these extremes. The float height values are an average of six independent measurements and would therefore have an rms error of $1/\sqrt{6}$ of these values.

c. Results of Flight 55P

We have only preliminary data analysis and results from this flight. The actual flight profile has not been received from the balloon base. Consequently, the brightness

temperatures are plotted against time (minutes after launch) rather than height. The float height is known to be 30.1 km. Monitored temperatures indicate the profile to be very similar to that of Flight 33P.

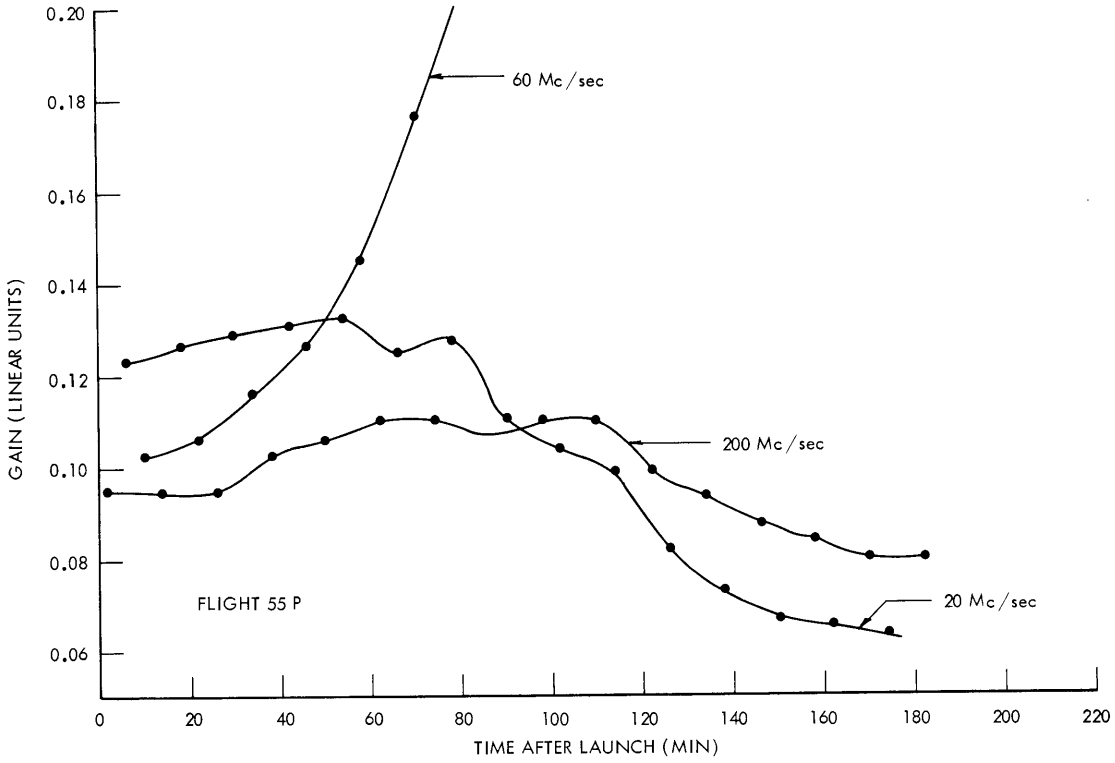

Fig. II-6. Amplifier gains. Flight 55P.

The gain of the channels versus time is shown in Fig. II-6. At 70 minutes the gain of the 60 Mc/sec amplifier had increased to the point where the tape recorder saturated for the corresponding calibration signals. Hence, useful data were obtained for the first 70 minutes from the 60-Mc/sec channels, and for the first 180 minutes from the 20-Mc/sec and 200-Mc/sec channels.

Figure II-7 shows the measured brightness temperatures plotted against time. For times less than 120 minutes (at which time the liquid nitrogen had evaporated) the rms error is ~5°K. After this time, the error increased to ~20°K because of uncertainties in the cold-load temperature.

The rms error of 5°K is due primarily to the method of data analysis. (The actual ΔT_{rms} for the radiometer channels is less than 2°K for each.) The minimum detectable difference on the chart paper is ~0.5 mm, which represents 5°K. A chart recording system with a larger dynamic range would allow this error to be decreased.

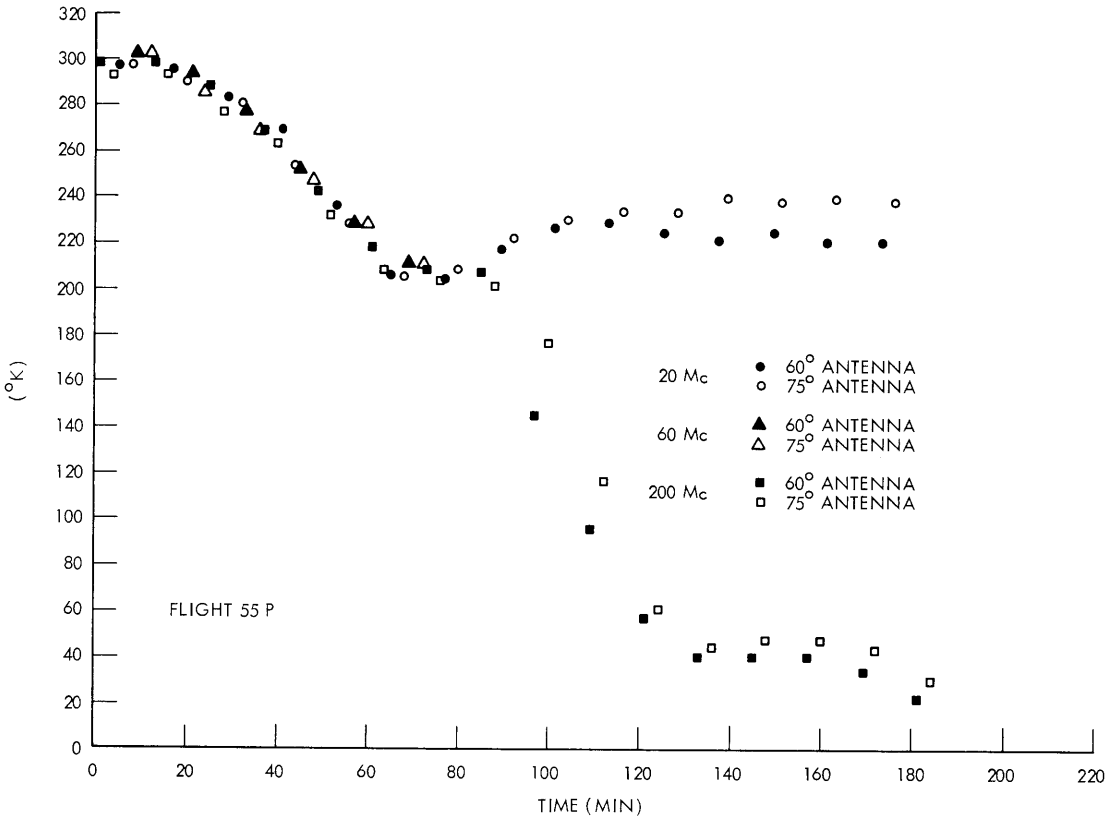

Fig. II-7. Brightness temperature vs time.

5. Future Plans

a. Immediate Plans

Plans have been made for two flights during the week of 19 October 1964. To improve the data recovery, a transmitter, as well as the tape recorder, will be flown with the radiometer. It is anticipated that the data for both flights will be successfully recovered and will have an rms error of approximately 2°K for each measurement.

Work is being done to find the kinetic temperature of the atmosphere between 30 and 100 km from the six brightness temperatures measured at the balloon float heights.

b. Plans after 1964

A primary objective of this program is to design and perfect spectral-line radiometers capable of operating at approximately 5-mm wavelength on spacecraft. The next step is to fly such a radiometer in a high-altitude (100 km) aircraft to observe the Earth at these wavelengths. This experiment should give results that would be similar to those expected from a satellite-borne experiment. Work has begun on this project.

Figure II-8 shows the theoretical brightness temperature across the 9^+ resonance

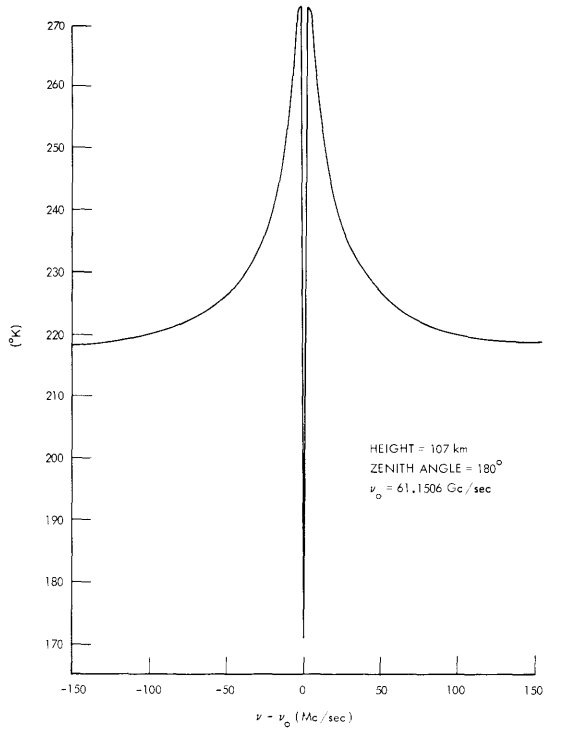

(a)

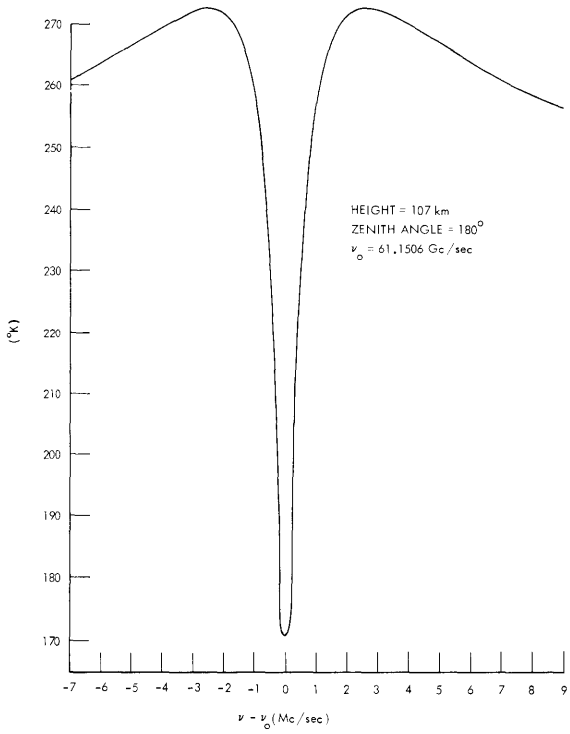

(b)

Fig. II-8. Brightness temperatures.

viewed from above at 107 km. In this calculation the Zeeman effect and Doppler broadening have been ignored.

The seemingly strange shape is due to the temperature profile of the atmosphere. On the wings (≈100 Mc off resonance) the opacity of the atmosphere is such that the radiometer "sees" deeply into the atmosphere (to ~20-30 km). At resonance, the opacity is very large so that the radiometer does not penetrate deeply (~80-90 km). For frequencies between these extremes the brightness temperature roughly follows the atmospheric temperature as the effective source height is increased.

Consideration of the Zeeman effect greatly complicates the simple picture. The one resonance is split into 19 different resonances and the splitting depends on the magnitude of the earth's magnetic field. Furthermore, the brightness temperature then depends on the polarization of the receiving apparatus.

A great simplification can be obtained by using the 1^+ line (ν_o=56.2648 Gc/sec) rather than the 9^+ line (ν_o=61.1506 Gc/sec). This simplification results from the fact that the magnetic field causes the 1^+ line to split into 3 components, rather than 19 components for the 9^+ line.

Preliminary work is being done to include the Zeeman effect in the theoretical calculations. Upon completion of this phase of the investigation an experiment appropriate to high-altitude aircraft (if available) observations will be planned and built.

6. Conclusions

Inasmuch as the data from Flight 55P have not been completely analyzed, only tentative conclusions can be made at this time.

The loss of the 60-Mc channel in Flight 55P prevents any interpretation concerning line shapes. The large rms errors associated with Flight 33P similarly limit its usefulness.

From Flight 55P results it can be concluded that the radiometer itself is operating quite well. In flights that will be made in October 1964 we expect that, with the transmitting apparatus included, the necessary data will be obtained. We can say now that the experimental measurements follow the theory approximately; however, conclusions regarding linewidth, intensity, and angular dependence of the observations will have to await further developments.

W. B. Lenoir, J. W. Kuiper

References

1. Quarterly Progress Report No. 71, Research Laboratory of Electronics, M. I. T., October 15, 1963, pp. 69-76.

B. LONG-WAVELENGTH RADIO ASTRONOMY IN SPACE

1. Introduction

It is most important for an understanding of the structure of our galaxy that we know its long-wavelength spectrum. In particular, the portion of the spectrum below 20 Mc should be mapped in detail. The long-wavelength limit of the terrestrial radio window is imposed by the ionospheric F_2 region and is approximately 20 Mc/sec. In general, one may say that frequencies lower than 20 Mc may not be accurately observed from the Earth's surface. It is desirable, then, to place radiometers above the ionosphere at an altitude exceeding 500 miles to eliminate this lower frequency limit. Measurements in space are at present being conducted by several experimenters[1-5] at frequencies ranging from 700 kc to 5 Mc in an initial effort to determine the total integrated cosmic flux density and local noise level. Results obtained thus far seem to have posed more problems than they have solved. They do indicate, however, that experiments are proceeding in the proper direction.

2. The Need for Improved Spatial Resolution

A major drawback of previous experiments was a lack of directivity in antenna pattern. At these low frequencies, any antenna that has been used thus far has been much shorter than a wavelength and therefore essentially omnidirectional. This is a serious problem, since it is supposed that there are high noise levels in the vicinity of the Earth,[1, 2] and there is no conclusive evidence to indicate that the fluxes measured to date are not composed largely of terrestrial noise from the radiation belts surrounding the Earth.[4] To resolve this problem and thus obtain accurate cosmic-noise measurements, two things must be accomplished. First, the satellites must be orbited above the noise-producing regions of the Earth's exosphere; and second, spatial resolution must be improved. We hope that the first will be solved by experiments now proposed such as those contained on the POGO and EGO satellites that will be launched in a year or two.[6] A solution to the second problem is presented below.

3. Interferometers in Space

Many proposals have been made for improving the spatial resolution of low-frequency radio-astronomy measurements, but none have yet been tried. The simplest, in theory, is the erection of long wire antennas several wavelengths long.[1] Other methods include V-beam antennas, ionospheric gradient focusing (IGF), and Z-mode propagation.[1, 4, 7] With the exception of the Z-mode, these techniques will not achieve a resolution greater

than approximately 20°; and 60° is a more common figure. It is doubtful whether Z-mode and IGF will yield any useful results at all if it is shown that there is a high terrestrial noise level, since, to obtain these focusing effects, orbits must be relatively low at approximately 600 km.

An alternative to these methods is an aperture synthesis method employing interferometric techniques. An interferometer system orbited in space could give resolution of 2° at a frequency of 1 Mc with a base line of approximately 8 km. Higher resolution could be obtained by simply extending the base line. Such a system would include two satellites orbiting together in such a way that the relative positions of the two could be controlled in a known manner either by gas jets on one of the satellites or by having them drift apart in a known manner. At present, we envision a master-slave system, with the master satellite containing the correlation equipment as well as the command and control links to earth and the slave. The slave would contain only an antenna, receiver, and suitable equipment for communication with the master but not with the ground. The slave could also contain gas jets and control circuitry for positioning if this method is used. Although an orbiting system is advisable for extended data collection, the preliminary measurements and testing could be done from rockets.

Signal processing and data communication between satellites would be greatly simplified by the use of clipped signals. The use of this method[8] would ease the stringent requirements of gain stability in the radiometers and the unknown path attenuation between satellites. The clipped-signal method also reduces the data rate and simplifies data handling and correlation procedures. By using aperture synthesis techniques in space, high-resolution maps of cosmic noise from the galaxy and other sources can be mapped to angular resolutions of ~1° at frequencies in the 100 kc-1 Mc range. An interesting point is that as the frequencies get lower, data handling and correlation are easier with this system, but for high-resolution measurements employing single antenna structures they become more difficult. The need for such a system has been suggested before.[9] We believe that our ideas represent a realistic and concrete approach to the problem.

R. K. Breon, J. W. Graham

References

1. G. R. Huguenin, Long-Wavelength Radio Astronomy in Space, HSRP-104, Harvard College Observatory, Cambridge, Mass., 1963.

2. D. Walsh, et al., Cosmic Radio Intensities at 1.225 and 2.0 Mc Measured up to an Altitude of 1700 km, Radio Astronomy Observatory, University of Michigan, Ann Arbor, Mich., 1963.

3. G. R. Huguenin, et al., Measurements of Radio Noise at 0.7 and 2.2 Mc from a High-Altitude Rocket Probe, HSRP-107, Harvard College Observatory, Cambridge, Mass., 1963.

4. M. D. Papagiannis, Natural Ionospheric Directivity and Measurements of Radio Radiation in Space, HSRP-108, Harvard College Observatory, Cambridge, Mass., 1964.

5. F. T. Davies, Alouette Topside Ionospheric Studies, I. G. Bulletin, January 1964.

6. Space Research and the IQSY, I. G. Bulletin, January 1963.

7. H. P. Palmer, R. D. Davies, and M. I. Farge (eds.), Radio Astronomy Today (Harvard University Press, Cambridge, Mass., 1963), Chap. 5.

8. R. K. Breon, Interferometers Using Clipped Signals, S. M. Thesis, Department of Electrical Engineering, M. I. T., May 1963.

9. A Review of Space Research, National Research Council Publication 1079, 1962, Chapter 2, Section V.

C. FOUR-MILLIMETER RADIO TELESCOPE

Work on our 4-mm radio telescope is continuing. A careful examination of the receiving antenna revealed a high side lobe (10 db) caused by distortions in the surface of the 10-foot parabolic reflector. Gain was 1 to 2 db below that anticipated. It appears that our present reflector is only marginally satisfactory for observations on large sources (the sun and moon) but will be useful on sources whose angular size is smaller than our 6-minute beamwidth. A study of pointing accuracy by using an astronomical refractor and visible stars is under way, and initial results indicate that this accuracy is well within a beamwidth.

We had intended to undertake Venus observations during June but equipment modifications, weather delays, and personnel limitations made this impossible.

J. W. Graham

D. THERMAL LOAD FOR RADIOMETER CALIBRATION

When making radio astronomy measurements it is necessary to calibrate the receiving system. One standard method of calibration is to place a matched load at a known temperature at the radiometer input and record the change in the output signal. This is the principle followed in this design of a calibration standard for the 72-Gc radiometer.

The thermal load is essentially a load with a VSWR = 1.15, which has been heated to a known temperature to within ±0.5°C. The major advantage of the design is the fact that the temperature change from the load to the output guide occurs over a very short section of stainless steel waveguide so that corrections to the source temperature (as seen looking into the waveguide) are minor. At 150°C this correction to the source temperature is about −0.1°C.

The thermal load will also be used to calibrate secondary gas standards (noise tubes) which are used for calibrations during observations.

1. Theory

Figure II-9 shows a diagram of the thermal load. The load is at a temperature T_L and the output flange is at room temperature T_o. With this configuration the source temperature T_s of the thermal load (as seen looking into the output guide), will depend on the temperature of the load T_L, the emission and attenuation of the output guide, and the VSWR of the load. First we will consider the effects of the emission and attenuation of the output guide.

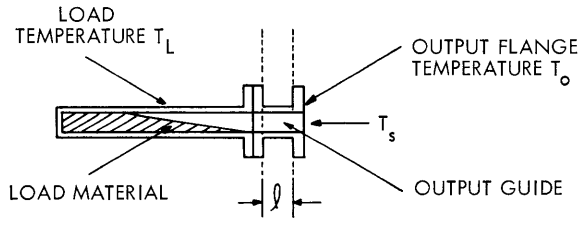

Fig. II-9. Diagram of matched load.

To account for the emission from the output guide it will be necessary to assume a temperature distribution along this guide. If the length ℓ of the output guide is short, we may assume a linear temperature distribution along the output guide with little error. If the attenuation constant of the output guide is γ, then the source temperature T_s due to emission and attenuation is given by

$$T_{s1} = \beta T_L + T_o(1-\beta),$$

where

$$\beta = \frac{1 - e^{-\gamma\ell}}{\gamma\ell}.$$

Now if $\gamma\ell \ll 1$, which implies a short length and low attenuation, we see

$$T_{s1} = T_L - \frac{\gamma\ell}{2}(T_L - T_o). \tag{1}$$

The second correction to the source temperature is added because of mismatch of the load. We may write the source temperature as

$$T_{s2} = T_L - |\Gamma|^2(T_L - T_i), \tag{2}$$

where T_i is the temperature of incident waves in system, and $|\Gamma|^2$ is the fraction of power reflected.

$$|\Gamma|^2 = \left(\frac{r-1}{r+1}\right)^2, \qquad \text{where } r = \text{VSWR}.$$

Taking into account both of the above effects we combine Eqs. 1 and 2 to get the corrected source temperature.

$$T_s = T_L - \frac{\gamma\ell}{2}(T_L - T_o) - |\Gamma|^2(T_L - T_i).$$

The corrected source temperatures and the corrections are tabulated below for the three thermal loads.

	Temperatures (°C)		
Load Temperature, T_L	50	100	150
Correction due to emission and attenuation in the output guide	-0.0352	-0.0975	-0.1625
Correction due to VSWR of the load	0.0	-0.125	-0.25
Corrected source temperature, T_s	50.0	99.8	149.7

The values used in these calculations are $\gamma = 0.52$ ($\alpha = 4.5$ db/m at 70 Gc for silver waveguide), $\ell = 0.5$ cm, VSWR = 1.15, $|\Gamma|^2 = 2.5 \times 10^{-3}$, $T_i = 50°C$, and $T_o = 25°C$.

2. Design

The thermal load has two separate sections, the actual matched load and waveguide, and the temperature control circuit, and these will be discussed in order. The load material was an iron-loaded resin (Echosorb MF117-500F, Emerson Cummings). This material was selected for its high temperature properties and low VSWR (~1.05) when tapered. The load was placed in a silver waveguide and this waveguide was placed in an oil-filled cannister with a Nichrome heater. In front of this combination, a stainless steel waveguide section (length 0.4 cm, wall thickness 0.010 in.) was placed to reduce the heat loss from the matched load. Actual heat loss was less than 0.6 watt. The inside walls of the stainless section were silver plated to reduce attenuation. The VSWR of the complete assembly was 1.15. This entire assembly was then enclosed in an insulated box. To maintain the temperature of the waveguide and the load at 150°C it was necessary to supply 4 watts of power to the heater.

The temperature control circuit consists of an AC bridge circuit (with a thermistor in one arm) that supplies a signal to a phase-sensitive amplifier that in turn controls the current to the heater in the waveguide cannister.

The control circuit has a capability of three fixed temperatures: 50°C, 100°C, 150°C and the short-term stability of the temperature is better than ±0.1°C. The temperature of the load is monitored with a separate measurement circuit (DC thermistor bridge) using a zero-center meter which reads zero when the correct temperature is reached.

The thermal load was calibrated by first determining the resistance of one thermistor very accurately at each of the desired temperatures. In this calibration, the thermistor was immersed in an oil bath whose temperature was known to ±0.1°C (using a calibrated thermometer) and then its resistance was measured with a Wheatstone bridge. This

thermistor was then mounted on the load waveguide and by using the internal heater to obtain the correct temperature (as determined by the resistance of the calibrated thermistor) the correct values of resistance were chosen to balance the bridge.

Considering all aspects of the calibration procedure, the absolute temperature of the load should be within ±0.5°C of the desired temperature. This accuracy can be maintained by periodically recalibrating the measurement circuit.

When calibrating a Dicke radiometer it is necessary to have two sources at known temperatures. Therefore a second thermal load is now being constructed using the same principles as the load just described. A few improvements, such as a lower temperature (0°C), less time between temperature changes, and smaller size have been incorporated.

W. J. Wilson